Systematical calculations on α-cluster preformation factors and decay half-lives of light nuclei near the recently observed α emitters ^{108}Xe and ^{104}Te

Niu Wan [1,2,*] and Jingya Fan [2]

[1] *School of Physics and Optoelectronics, South China University of Technology, Guangzhou 510641, China*

[2] *School of Physics, Nanjing University, Nanjing 210093, China*

(Received 16 September 2021; accepted 10 December 2021; published 22 December 2021)

In this paper, we systematically calculate the α-cluster preformation factors and decay half-lives of light nuclei around two newly observed self-conjugate emitters ^{108}Xe and ^{104}Te. The cluster-formation model is employed to calculate the preformation factors by using the experimental nuclear binding energies obtained from the recently updated atomic mass evaluation (AME2020). The binding energies calculated by the improved Weizsäcker-Skyrme formula (WS4) are also used to evaluate the preformation factors. The typical behaviors are obtained that the preformation factors of even-even nuclei are larger than those of odd-*A* (even-odd and odd-even) nuclei and the latter are generally larger than those of odd-odd nuclei. Besides, due to Pauli blocking, the preformation factors for isotopic chains are decreased with the increasing neutron number. However, it is found that, as a result of the competition between the Pauli blocking and Coulomb repulsion effects for isotonic chains, the preformation factors are generally increased with the increasing proton number. Moreover, with these obtained preformation factors, the α-decay half-lives of these light emitters are further calculated under the density-dependent cluster model. The calculated results are compared with experimental data, especially for the two newly observed emitters.

DOI: 10.1103/PhysRevC.104.064320

I. INTRODUCTION

One of the fundamental nuclear decay modes is α decay, which manifests by emitting an α cluster from the parent nucleus. The mechanism of α decay was successfully explained in 1928 for the first time by Gamow [1] and Condon *et al.* [2] as a pure quantum tunneling effect. After these pioneering works, different theoretical models have been subsequently established to study the properties of α decays [3–14]. The α-decay process is usually described as a preformed α cluster in the parent nucleus penetrating the Coulomb barrier of the total interaction between the α cluster and the daughter nucleus. The α-decay width is closely related to the α-cluster preformation probability P_α (preformation factor) and the barrier penetration probability. The latter is exponentially dependent on the so-called Gamow factor [1], which can be readily calculated. However, the thorough calculation of the former P_α involves a complicated many-body problem, in which the preformation factor is generally treated as the overlap between the initial state of the parent nucleus and the final states of the outgoing α cluster and the daughter nucleus. There are several studies to directly calculate the α-cluster preformation factors. For example, by combining the shell and cluster models, Varga *et al.* successfully calculated the preformation factor $P_\alpha = 0.23$ for the nucleus ^{212}Po with an α cluster plus a doubly magic core ^{208}Pb [15]. With some reasonable approximations for the many-body system, the preformation factors in heavy and superheavy nuclei can be microscopically calculated in the quarteting wave-function approach [16–20]. By analyzing the interactions among the valence nucleons in the parent nucleus, Ahamed *et al.* proposed a cluster-formation model (CFM) to study the α clustering [21–24], where the experimental separation energies are used to calculate the preformation factor P_α instead of solving the many-body problem. The CFM has been used to systematically calculate the α-cluster preformation factors for heavy and superheavy nuclei [21–24]. The calculated preformation factor for ^{212}Po is about $P_\alpha = 0.221$ [21], which is consistent with previous microscopic calculations.

Allowing for the complication of the microscopic calculations, the preformation factors P_α in many previous studies are usually assumed to be constant or extracted by reproducing the experimental α-decay half-life. From this simplicity, there have been several different models proposed to calculate the α-decay half-lives throughout the nuclide chart. For instance, Buck *et al.* performed systematic calculations of α-decay half-lives [25–27] within a realistic potential and the two-potential approach (TPA) [28]. By using the generalized liquid-drop model [29], Royer *et al.* systematically computed the half-lives of α emitters. With the stationary coupled channels approach, Delion and coworkers analyzed many α decays into both ground and excited states [30,31]. Under the density-dependent cluster model (DDCM) [32–41], the α-decay half-lives for both spherical and deformed emitters are investigated. By using the Coulomb and proximity potential model for deformed nuclei, Santhosh *et al.* studied the α-decay properties of heavy and superheavy emitters

*wanniu@scut.edu.cn

[42–44]. Recently, the relativistic energy density functional is also used to study the α-decay properties by including the nuclear deformations [45].

The majority of α-cluster emitters are located in the region of heavy and superheavy nuclei. However, there also exist some lighter nuclei with spontaneous α decays in the vicinity of the doubly magic nucleus ^{100}Sn with $N = Z = 50$ [46–49]. Different experiments have been conducted to investigate the α-decay properties in this region, especially for searching the potential superallowed α decays [50–55]. Recently, the new α-decay chain $^{108}\text{Xe} \rightarrow {}^{104}\text{Te} \rightarrow {}^{100}\text{Sn}$ was reported by the Argonne National Laboratory (ANL) [54]. This is not only the first time to observe an α decay into a self-conjugate core ^{100}Sn but also the second case decaying into a doubly magic daughter nucleus. From the available experimental data, they deduced the half-lives of $T_{1/2} = 58^{+106}_{-23}$ μs for ^{108}Xe and $T_{1/2} < 18$ ns for ^{104}Te, making the latter the new fastest α-cluster emitter. A subsequent experiment designed for searching this new α-decay chain observed two events, and the data would lead to a smaller half-life $T_{1/2} < 4$ ns for ^{104}Te and further experiments are suggested for conclusive measurements [55].

The α decays of these light emitters are of particular importance to study the structure and properties of nuclei approaching the $N = Z$ line as well as the shell effect around the $Z = N = 50$. The studies on the decay properties of light α-cluster emitters are attracting more and more attention. In this paper, we employ the CFM to calculate the α-cluster preformation factors. By using the obtained preformation factors, the α-decay half-lives of these light emitters are further calculated within the DDCM. This paper is organized as follows: In Sec. II, the frameworks of CFM and DDCM are introduced. In Sec. III, the α-cluster preformation factors and decay half-lives of light emitters are calculated and discussed. A summary is given in Sec. IV.

II. FORMALISM

A. Cluster-formation model

The α-decay process is usually treated as a two-body system with a preformed α cluster and a daughter nucleus inside the mother nucleus. The Hamiltonian of the clustering state can be denoted as $H = H_f + H_r$ [21,22], where H_f is the Hamiltonian for the cluster-formation state and H_r describes the relative motion between the preformed cluster and the daughter nucleus. As discussed in Refs. [21–24], the cluster preformation factor can be calculated by

$$P_f = \frac{\langle \Psi | H_f | \Psi \rangle}{\langle \Psi | H_f | \Psi \rangle + \langle \Psi | H_r | \Psi \rangle}, \tag{1}$$

where $\Psi = \Phi_f \cdot \Phi_r$ is the total wave function with Φ_f for the cluster-formation state and Φ_r for the relative motion. They satisfy the corresponding time-independent Schrödinger equations

$$H_f \Phi_f = E_f \Phi_f, \tag{2}$$

$$H_r \Phi_r = E_r \Phi_r, \tag{3}$$

where E_f is the eigenvalue of the cluster-formation energy and E_r is the energy for the relative motion. By using above two relations, Eq. (1) can be rewritten as

$$P_f = \frac{\langle \Phi_f | H_f | \Phi_f \rangle}{\langle \Phi_f | H_f | \Phi_f \rangle + \langle \Phi_r | H_r | \Phi_r \rangle}. \tag{4}$$

With respect to the α clustering, by inserting Eqs. (2) and (3) into Eq. (4), the corresponding α-cluster preformation factor can be denoted [21–24]

$$P_\alpha = \frac{E_{f\alpha}}{E_{f\alpha} + E_r} = \frac{E_{f\alpha}}{E}, \tag{5}$$

where $E_{f\alpha}$ is the α-cluster-formation energy originating from the interactions among the four nucleons in the α clustering and E_r is the energy for the relative motion between the four nucleons and the residual nucleons in the daughter nucleus. The quantity $E = E_{f\alpha} + E_r$ is the total energy for the α-clustering state which satisfies $H\Psi = E\Psi$. If the α-core interaction is very large, namely $E_r \gg E_{f\alpha}$, the preformation factor P_α approaches zero, which indicates that the interactions among the four nucleons in the α clustering are very minor and the α clustering hardly preforms. On the contrary, if the interactions among the four nucleons in the α clustering are significant, namely $E_{f\alpha} \gg E_r$, the preformation factor P_α will approach unity, which corresponds to full α clustering. In principle, in order to calculate the preformation factor, the two energies $E_{f\alpha}$ and E in Eq. (5) should be calculated by solving the corresponding Schrödinger equation. However, as discussed in previous works [21–24], by analyzing the surface nucleon-nucleon interactions, above two energies can both be approximately calculated from the experimental separation energies [23,24]

$$E_{f\alpha} = \begin{cases} 2S_p + 2S_n - S_\alpha & \text{(even-even)} \\ 2S_p + S_{2n} - S_\alpha & \text{(even-odd)} \\ S_{2p} + 2S_n - S_\alpha & \text{(odd-even)} \\ S_{2p} + S_{2n} - S_\alpha & \text{(odd-odd),} \end{cases} \tag{6}$$

$$E = S_\alpha(A, Z), \tag{7}$$

where S_p, S_n, S_{2p}, S_{2n}, and S_α are one-proton, one-neutron, two-proton, two-neutron, and α-cluster separation energies, respectively. They can be calculated by the difference of the relevant binding energies [56–58]:

$$S_p(A, Z) = B(A, Z) - B(A - 1, Z - 1), \tag{8}$$

$$S_n(A, Z) = B(A, Z) - B(A - 1, Z), \tag{9}$$

$$S_{2p}(A, Z) = B(A, Z) - B(A - 2, Z - 2), \tag{10}$$

$$S_{2n}(A, Z) = B(A, Z) - B(A - 2, Z), \tag{11}$$

$$S_\alpha(A, Z) = B(A, Z) - B(A - 4, Z - 2), \tag{12}$$

where $B(A, Z)$ is the binding energy of a nucleus with mass number A and proton number Z. The majority of the experimental binding energies can be directly obtained from the recently updated atomic mass evaluation table (AME2020) [56–58]. However, there are no experimental data for some very special cases involved in Eqs. (8)–(12), such as ^{102}Te and ^{103}Te. Fortunately, due to the effort of the community, there have been different nuclear mass formulas [59–65] proposed

to not only accurately reproduce the masses (binding energies) of nuclei throughout the nuclide chart but also predict binding energies of nuclei without experimental data. By using the improved Weizsäcker-Skyrme formula (WS4) [65], Wang *et al.* reproduced the experimental masses of all the 2353 nuclei with a root-mean-square derivation less than 0.3 MeV, which has been one of the most accurate calculations up to now. Therefore, besides of the AME2020, we will also use the binding energies obtained from WS4 to calculate the α-cluster preformation factors, especially for nuclei without experimental data.

B. Density-dependent cluster model

The light α-cluster emitters are mainly located in the medium-mass region, where the nuclei usually involve deformations. Within the framework of DDCM including the nuclear deformation effect, the total α-core interaction can be written as the summation of nuclear, Coulomb, and centrifugal potentials [33–38]:

$$V_T(R,\beta) = V_N(R,\beta) + V_C(R,\beta) + \frac{\hbar^2}{2\mu}\frac{\ell(\ell+1)}{R^2}, \tag{13}$$

where R is the distance between the mass center of the α cluster and that of the daughter nucleus. The parameter β is the orientation angle of the α cluster with respect to the symmetry axis of the daughter nucleus. The nuclear and Coulomb potentials can be obtained from the double-folding procedure [66–68]

$$V_N(R,\beta) = \lambda \int d\mathbf{r}_1 d\mathbf{r}_2 \rho_1(\mathbf{r}_1)\rho_2(\mathbf{r}_2) g(s,\varepsilon), \tag{14}$$

$$V_C(R,\beta) = \int d\mathbf{r}_1 d\mathbf{r}_2 \rho_{1p}(\mathbf{r}_1)\frac{e^2}{s}\rho_{2p}(\mathbf{r}_2), \tag{15}$$

where the quantity $s = |\mathbf{R} + \mathbf{r}_2 - \mathbf{r}_1|$ is the distance between a nucleon in the α cluster and one in the daughter nucleus. The function $g(s,\varepsilon) = 7999\frac{e^{-4s}}{4s} - 2134\frac{e^{-2.5s}}{2.5s} - 276(1-0.005\varepsilon)\delta(s)$ with $\varepsilon = Q/A_1$ is the M3Y effective nucleon-nucleon (NN) interaction [66–68]. The quantity Q is the α-decay energy and $A_1 = 4$ is the mass number of the α cluster. The quantities $\rho_1(\mathbf{r}_1)$ and $\rho_{1p}(\mathbf{r}_1)$ are, respectively, the total and proton density distributions of the α cluster with the standard Gaussian form from electron scattering [67,68]: $\rho_1(r_1) = 0.4229\exp(-0.7024r_1^2)$. Similarly, $\rho_2(\mathbf{r}_2)$ and $\rho_{2p}(\mathbf{r}_2)$ are the total and proton density distributions of the daughter nucleus, respectively. Considering the deformation of the daughter nucleus, the density distribution $\rho_2(\mathbf{r}_2)$ within the two-parameter Fermi form can be written as [33–35]

$$\rho_2(r_2,\theta) = \frac{\rho_{20}}{1+\exp\left[\frac{r_2 - R(\theta)}{a}\right]}, \tag{16}$$

where ρ_{20} is a normalization factor by integrating the total density distribution equal to the mass number A_2 of the daughter nucleus. The half-density radius $R(\theta)$ is given as $R(\theta) = R_0[1 + \beta_2 Y_{20}(\theta) + \beta_4 Y_{40}(\theta)]$, where β_2 and β_4 are the quadrupole and hexadecapole deformation parameters, respectively. Their values can be obtained from the nuclear deformation table [64]. The parameter $R_0 = 1.07A_2^{1/3}$ fm and the diffuseness parameter $a = 0.54$ fm are taken from Refs. [69–71].

The parameter λ in Eq. (14) is the strength of the nuclear potential, which can be determined by employing the Bohr-Sommerfeld quantization condition [10,25–27]

$$\frac{1}{2}\int_0^{\pi}\int_{R_1(\beta)}^{R_2(\beta)} \sqrt{\frac{2\mu}{\hbar^2}|V_T(R,\beta) - Q|}\sin\beta dR d\beta = (G - \ell + 1)\frac{\pi}{2}, \tag{17}$$

where $R_1(\beta)$, $R_2(\beta)$, and the following $R_3(\beta)$ are the three classical turning points, respectively, which are obtained from $V_T(R,\beta) = Q$. The global quantum number G in Eq. (17) is given by [25]

$$\begin{aligned} &G = 22 \quad (N > 126), \quad G = 20 \quad (82 < N \leqslant 126), \\ &G = 18 \quad (N \leqslant 82). \end{aligned} \tag{18}$$

After determining the strength parameter λ, the total interaction in Eq. (13) can be obtained. Then the angle-dependent α-cluster penetration probability can be calculated by [33–35]

$$P_\beta = \exp\left[-2\int_{R_2(\beta)}^{R_3(\beta)}\sqrt{\frac{2\mu}{\hbar^2}|V_T(R,\beta) - Q|}dR\right]. \tag{19}$$

The total penetration probability P_T can be obtained by averaging P_β in all directions as $P_T = \frac{1}{2}\int_0^{\pi} P_\beta \sin\beta d\beta$. By using the two-potential approach [28], the α-decay width can be calculated by [33–35]

$$\Gamma = P_\alpha F \frac{\hbar^2}{4\mu}\frac{1}{2}\int_0^{\pi} P_\beta \sin\beta d\beta, \tag{20}$$

where P_α is the α-cluster preformation factor and F is a normalization factor, which is well defined by the TPA [28]. If the value of the latter is close to unity, it describes a good quasiclassical bound-state approximation for α decay. It can be obtained similarly by averaging along different orientation angles as $F = \frac{1}{2}\int_0^{\pi} F_\beta \sin\beta d\beta$ [33–35], where F_β is the angle-dependent factor and can be calculated by [28]

$$F_\beta \int_{R_1(\beta)}^{R_2(\beta)} \frac{dR}{2\sqrt{\frac{2\mu}{\hbar^2}|V_T(R,\beta) - Q|}} = 1. \tag{21}$$

In this work, the values of the normalization factor are in the range of 0.82–0.89, indicating the reliability of present calculations. Consequently, we can obtain the α-decay half-life by the well-known relation to the decay width $T_{1/2} = \hbar \ln 2/\Gamma$.

III. RESULTS AND DISCUSSION

In Table I, we list the calculated α-cluster preformation factors P_α and decay half-lives of the light parent nuclei around the two newly observed emitters ^{108}Xe and ^{104}Te. Shown in the sixth and seventh columns of Table I are the preformation factors calculated by the binding energies obtained from the mass tables AME2020 [56–58] and WS4 [65], respectively. To check the validity of the WS4 results, we calculate the

TABLE I. Calculated values of α-cluster preformation factors P_α and decay half-lives $T_{\rm calc.}$ of light parent nuclei around ^{108}Xe and ^{104}Te. The preformation factors calculated by the binding energies obtained from the AME2020 [56–58] and WS4 [65] mass tables are both presented. The experimental data of the α-decay energies Q_α and half-lives $T_{\rm expt.}$ are also taken from AME2020. The deformation parameters β_2 and β_4 are taken from the nuclear deformation table [64]. The decay energies and half-lives of the two newly observed emitters ^{108}Xe and ^{104}Te are taken from the recent ANL experimental paper [54].

Emitter	Q_α (MeV)	ℓ	β_2	β_4	$P_\alpha^{\rm AME}$	$P_\alpha^{\rm WS4}$	λ	$T_{\rm expt.}$ (s)	$T_{\rm calc.}$ (s)
Even-even									
^{104}Te	5.100	0	0.000	0.000	/	0.305	0.729	$<4.000\times10^{-9}$	5.387×10^{-8}
^{106}Te	4.290	0	0.000	0.000	0.247	0.261	0.725	7.800×10^{-5}	1.006×10^{-4}
^{108}Te	3.420	0	0.000	0.000	0.255	0.265	0.721	4.286×10^{0}	5.100×10^{0}
^{110}Te	2.699	0	0.000	0.000	0.239	0.246	0.717	/	2.101×10^{6}
^{108}Xe	4.600	0	0.000	0.000	/	0.332	0.721	7.200×10^{-5}	4.283×10^{-5}
^{110}Xe	3.872	0	0.119	0.066	0.258	0.279	0.719	1.453×10^{-1}	1.393×10^{-1}
^{112}Xe	3.330	0	0.139	0.056	0.276	0.254	0.715	2.250×10^{2}	3.440×10^{2}
^{114}Ba	3.592	0	0.173	0.063	0.271	0.255	0.714	5.111×10^{1}	1.049×10^{2}
Even-odd									
^{105}Te	5.069	2	−0.011	0.000	/	0.173	0.751	6.330×10^{-7}	2.397×10^{-7}
^{107}Te	4.010	2	0.000	0.000	0.109	0.150	0.748	4.600×10^{-3}	7.915×10^{-3}
^{109}Te	3.198	0	0.000	0.000	0.128	0.148	0.718	1.128×10^{2}	2.911×10^{2}
^{109}Xe	4.217	2	0.086	0.051	/	0.190	0.747	1.300×10^{-2}	7.523×10^{-3}
^{111}Xe	3.710	2	0.128	0.068	0.106	0.156	0.742	7.115×10^{0}	4.097×10^{0}
^{113}Xe	3.087	0	0.139	0.044	0.137	0.137	0.712	/	4.131×10^{4}
Odd-even									
^{109}I	3.918	2	0.086	0.051	0.130	0.173	0.744	6.629×10^{-1}	7.094×10^{-2}
^{111}I	3.275	0	0.117	0.042	0.135	0.142	0.715	2.841×10^{3}	3.429×10^{2}
^{113}I	2.707	0	0.128	0.031	0.138	0.130	0.710	1.994×10^{7}	1.565×10^{7}
Odd-odd									
^{108}I	4.099	2	0.075	0.051	0.094	0.088	0.748	2.653×10^{-2}	1.685×10^{-2}
^{110}I	3.580	2	0.107	0.053	0.070	0.079	0.743	3.906×10^{0}	1.273×10^{1}
^{112}I	2.957	4	0.117	0.042	0.063	0.057	0.741	2.783×10^{5}	3.439×10^{6}
^{112}Cs	3.930	0	0.150	0.071	/	0.086	0.715	$>1.885\times10^{-1}$	7.511×10^{-1}
^{114}Cs	3.360	0	0.173	0.049	0.065	0.066	0.711	3.167×10^{3}	3.350×10^{3}

χ^2-test value by

$$\chi^2/n = \frac{1}{n}\sum_i^n \frac{\left[P_\alpha^{\rm WS4} - P_\alpha^{\rm AME}\right]^2}{P_\alpha^{\rm AME}} \tag{22}$$

between these two sets of preformation factors. The value of χ^2/n is only about 0.004, which indicates that the $P_\alpha^{\rm WS4}$ values are in good agreement with the $P_\alpha^{\rm AME}$ values. Therefore, we can also expect the reliability of the obtained preformation factors $P_\alpha^{\rm WS4}$ for those nuclei without experimental energy data.

As shown in Table I, within the framework of CFM, the values of the preformation factors are all less than unity. Moreover, we obtain the typical behavior that the preformation factors in even-even nuclei (>0.2) are commonly larger than those in odd-A (even-odd and odd-even) nuclei (0.1–0.2), and the latter ones are usually larger than those in odd-odd nuclei (<0.1). The similar behavior is also obtained in previous systematical studies on α decays of heavy nuclei [21–27,33–35]. It is easy to understand this behavior that compared with even-even nuclei, there exist unpaired nucleons in even-odd and odd-even nuclei. Due to the Pauli blocking effect, these unpaired nucleons can result in hindrances to the formation of α cluster by reducing the amount of α clustering in the initial wave function. As a result, the overlap for the α clustering between the initial and final states will be decreased, leading to a smaller preformation factor. As for the odd-odd nuclei, the hindrances from the unpaired proton and unpaired neutron are much more remarkable, resulting in the smallest magnitudes of preformation factors. To show more details, we plot the α-cluster preformation factors P_α for isotopes with proton number $Z = 52$–55 and isotones with neutron number $N = 54$–59 in Figs. 1 and 2, respectively.

As shown in Fig. 1, the preformation factors P_α in each panel with even N are larger than those with odd N, which is the consequence of the unpaired neutron. Moreover, by comparing the results between $Z = 52, 54$ and $Z = 53, 55$, we can find that the preformation factors P_α for the isotopes with even Z are also usually larger than those with odd Z, which indicates that the paired protons contribute to the α clustering as well. Besides, there is a common feature that for each isotopic chain, the preformation factor P_α is generally decreased with the increasing neutron number N. This is because with the neutron number away from the neutron major shell $N = 50$, there will be more valence neutrons, leading to a stronger Pauli blocking effect on the α clustering and a smaller preformation factor.

Shown in Fig. 2 are the preformation factors for isotones with neutron number $N = 54$–59. Similar to the results for isotopes, in each panel the preformation factors with even Z

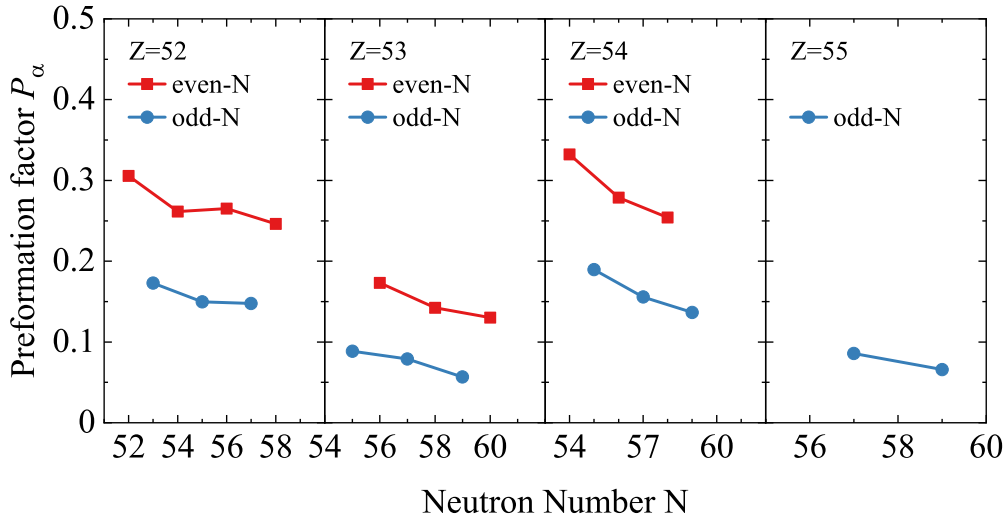

FIG. 1. α-cluster preformation factors P_α varied with neutron number N of parent nuclei for different isotopic chains.

are commonly larger than those with odd Z. Compared with the values between $N = 54, 56, 58$ and $N = 55, 57, 59$, the similar conclusion can be drawn that the preformation factors with even N are usually larger than those with odd N. These two typical features are also due to the Pauli blocking effect originating from the unpaired nucleons.

By comparing the results in Figs. 1 and 2, we can see an obvious difference between the isotopes and isotones. Opposite to the isotopes, the preformation factors P_α for the isotones in Fig. 2 are generally increased with the increasing proton number Z. This difference is also found in previous investigations for nuclei around ^{208}Pb [23,24,35–37]. However, it is difficult to explain the reason in heavy nuclei because of the possible configuration mixing of cross-shell excitations [72,73]. Different from heavy nuclei, the protons and neutrons in the light α-cluster emitters around ^{100}Sn are expected to occupy the same orbitals [46]. The main difference between the protons and neutrons in these light emitters is the charges carried by protons, which contribute to the α clustering and result in such opposite behavior for the isotones. In detail, for each isotonic chain for even Z or odd Z, when there are additional two paired-protons in the core, the Pauli blocking effect on the α clustering will become stronger. At the same time, the Coulomb repulsion effect which contributes to the α clustering between the charged α cluster and the core also becomes stronger. Although the stronger Pauli blocking effect can further hinder the α clustering, the additional Coulomb repulsion effect dominates, leading to larger preformation factors.

Moreover, by comparing the results between even Z and odd Z for the isotonic chain with $N = 57$ in Fig. 2, we can find that if only one proton is added such as from $Z = 52$ to $Z = 53$ and from $Z = 54$ to $Z = 55$, the preformation factor will be decreased. This is because, compared with adding a pair of protons, the additional unpaired proton can contribute more to the Pauli blocking effect than to the Coulomb repulsion effect, leading to smaller preformation factors. It is apparent that when two paired protons are added, such as from

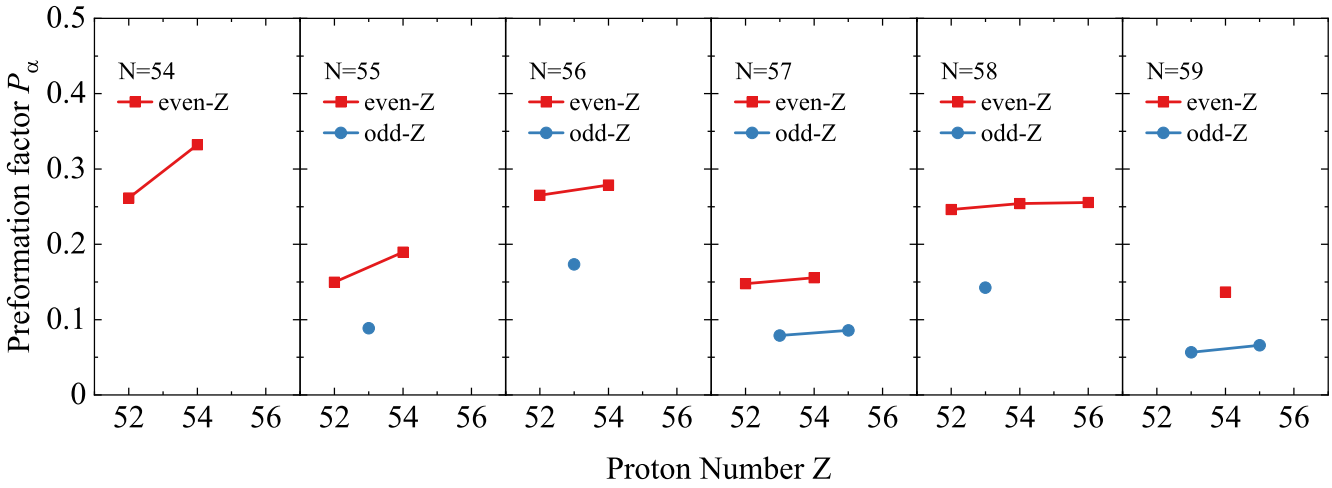

FIG. 2. α-cluster preformation factors P_α varied with proton number Z of parent nuclei for different isotonic chains.

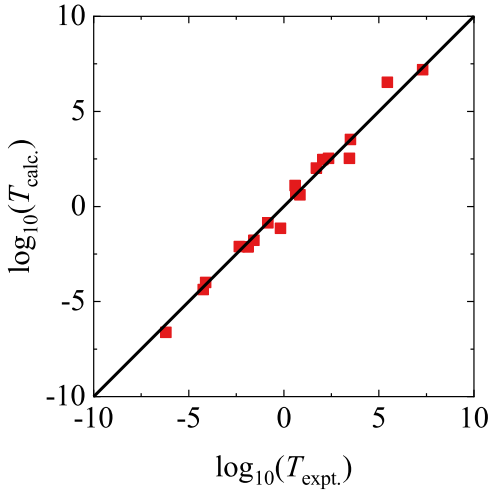

FIG. 3. Comparison between the calculated α-decay half-lives and the experiment data.

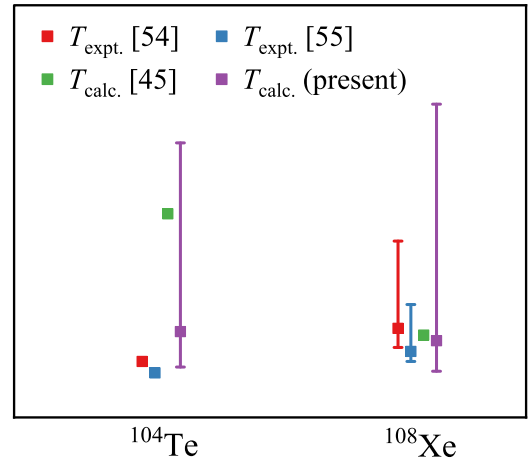

FIG. 4. Comparison of the theoretical and experimental half-lives for ^{108}Xe and ^{104}Te.

$Z = 52$ to $Z = 54$, the preformation factor will be increased due to the dominant Coulomb repulsion effect and smaller Pauli blocking effect.

Furthermore, compared with the results for $N = 54, 56, 58$ in Fig. 2, it can be seen that the climb of the preformation factor from $Z = 52$ to $Z = 54$ becomes moderate with the increasing neutron number. This is because, with the same number of protons, the Coulomb repulsion effect is very similar but the Pauli blocking effect becomes stronger with additional neutrons. As a result, the preformation factor gain becomes smaller. Therefore, the striking feature of the preformation factors for isotonic chains is the consequence of the competition between the Pauli blocking and Coulomb repulsion effects. The specific mechanism for this striking feature is of particular interest to be further microscopically investigated in the future.

With above-obtained preformation factors P_α^{WS4}, we further calculate the decay half-lives of these light emitters within the framework of the DDCM. In the last two columns of Table I, we present the experimental and theoretical α-decay half-lives for these light emitters, respectively. It can be seen that the magnitudes of the calculated decay half-lives are consistent with the experimental data. In Fig. 3, we plot the relation between the theoretical and experimental half-lives. It is obvious that all the points are very close to the $T_{\text{calc.}} = T_{\text{expt.}}$ line, which indicates that our theoretical half-lives agree with the experimental data. This fact also indicates the validity of the calculated α-cluster preformation factors.

In Table II, we present the calculated decay half-lives for the two newly observed emitters ^{108}Xe and ^{104}Te. The experimental decay energies Q_α are taken from the recent experimental paper [54]. For ^{108}Xe, the experimental half-life is measured as $T_{\text{expt.}} = 58^{+106}_{-23}$ μs, while only an upper limit $T_{\text{expt.}} < 18$ ns can be concluded for ^{104}Te [54]. A subsequent experiment also searched these two decays and the half-life $T_{\text{expt.}} = 30^{+57}_{-12}$ μs is deduced for ^{108}Xe. The corresponding data for ^{104}Te would lead to a smaller one $T_{\text{expt.}} < 4$ ns and further experiments are suggested for conclusive measurements [55]. In the newly updated mass table AME2020 [56], the half-life $T_{\text{expt.}} = 72 \pm 35$ μs is adopted for ^{108}Xe by averaging the above two experimental data. In a recent work, the relativistic energy density functional is used to study the properties of these two new emitters [45] and their half-lives are calculated to be $T_{\text{calc.}} = 50$ μs for ^{108}Xe and $T_{\text{calc.}} = 197$ ns for ^{104}Te, respectively. In the present work, by including the error bars of the experimental decay energies Q_α, the calculated decay half-lives are $T_{\text{calc.}} = 43^{+287}_{-37}$ μs for ^{108}Xe and $T_{\text{calc.}} = 54^{+229}_{-43}$ ns for ^{104}Te. Shown in Fig. 4 is the comparison of the theoretical and experimental decay half-lives for the two newly observed emitters. It can be clearly seen from Fig. 4 that the two theoretical calculations for ^{108}Xe are in good agreement with the experimental data, while both the

TABLE II. Calculated decay half-lives for the two newly observed emitters ^{108}Xe and ^{104}Te by including the error bars of the experimental decay energies Q_α.

Emitter	Q_α	$T_{\text{expt.}}$	$T_{\text{calc.}}$	$T_{\text{calc.}}$ (present)
^{108}Xe	4.6 $\pm$ 0.2 MeV [54]	58^{+106}_{-23} μs [54] 30^{+57}_{-12} μs [55] 72 $\pm$ 35 μs [56]	50 μs [45]	43^{+287}_{-37} μs
^{104}Te	5.1 $\pm$ 0.2 MeV [54]	<18 ns [54] <4 ns [55]	197 ns [45]	54^{+229}_{-43} ns

theoretical and experimental results for ^{104}Te still retain large uncertainty. By including the error bar of the experimental decay energy Q_α for ^{104}Te, the calculated decay half-life in present work is comparable with the experimental data. In the future, more investigations can be further conducted for the α-decay properties of these light emitters in both theoretical and experimental sides, especially for the new emitter ^{104}Te.

IV. SUMMARY

In this paper, we investigate the α-decay properties of light nuclei around the two newly observed self-conjugate emitters ^{108}Xe and ^{104}Te. By using the cluster-formation model (CFM), we systematically calculate the α-cluster preformation factors P_α of these light emitters. Both the experimental nuclear binding energies from AME2020 and theoretical energies from WS4 mass table are employed to calculate the preformation factors. The obtained preformation factors for WS4 agree very well with those for AME2020, which validates the calculated preformation factors for some special emitters such as the two new emitters.

From the calculations we find the typical behaviors of the preformation factors: due to the Pauli blocking effect, the preformation factors P_α for even-even nuclei are commonly larger than those for odd-A (even-odd and odd-even) nuclei, and the latter ones are generally larger than those for odd-odd nuclei. Besides, by comparing the results among different isotopic chains, we find that the preformation factors with even proton numbers are generally larger than those with odd proton numbers, which is also the result of the Pauli blocking effect. Similarly, for each isotopic chain, the preformation factors with even neutron numbers are generally larger than those with odd neutron numbers. These two behaviors are also found from the results for isotonic chains. Furthermore, from the calculations we find opposite features between isotopes and isotones. Because of the Pauli blocking effect for each isotopic chain, the preformation factors are generally decreased with the increasing neutron number. On the contrary, the preformation factors for each isotonic chain are generally increased with the increasing proton number, which is due to the competition of the Pauli blocking and Coulomb repulsion effects. By comparing the results for different isotonic chains, we find that the preformation factor gains become moderate, which also indicates the competition of above two effects for the striking opposite behavior.

With these obtained preformation factors, the decay half-lives of these light emitters are further calculated within the density-dependent cluster model (DDCM). The theoretical calculations are consistent with the experimental data. In particular, we compare the theoretical and experimental half-lives for the two new self-conjugate emitters ^{108}Xe and ^{104}Te. For ^{108}Xe, the theoretical calculations are in good agreement with the experimental data. By including the error bar of the experimental decay energy, the calculated decay half-life for ^{104}Te in present work is comparable with the experimental data.

ACKNOWLEDGMENTS

This work is supported by the National Natural Science Foundation of China (Grant No. 11822503) and the startup funding of South China University of Technology (Grant No. D6214030).

[1] G. Gamow, Eur. Phys. J. A **51**, 204 (1928).
[2] R. W. Gurney and E. U. Condon, Nature (London) **122**, 439 (1928).
[3] K. Varga, R. G. Lovas, and R. J. Liotta, Nucl. Phys. A **550**, 421 (1992).
[4] G. Royer, J. Phys. G **26**, 1149 (2000).
[5] D. S. Delion, Phys. Rev. C **80**, 024310 (2009).
[6] V. Yu. Denisov and A. A. Khudenko, Phys. Rev. C **81**, 034613 (2010).
[7] K. P. Santhosh and J. G. Joseph, Phys. Rev. C **86**, 024613 (2012).
[8] J. O. Rasmussen, Nucl. Phys. **44**, 93 (1963).
[9] D. N. Poenaru, M. Ivascu, and A. Sandulescu, J. Phys. G: Nucl. Phys. **5**, L169 (1979).
[10] B. Buck, A. C. Merchant, and S. M. Perez, Phys. Rev. C **45**, 2247 (1992).
[11] P. Mohr, Phys. Rev. C **73**, 031301(R) (2006).
[12] W. M. Seif, N. V. Antonenko, G. G. Adamian, and H. Anwer, Phys. Rev. C **96**, 054328 (2017).
[13] M. Ismail and A. Adel, Phys. Rev. C **97**, 044301 (2018).
[14] D. S. Delion and A. Dumitrescu, Phys. Rev. C **102**, 014327 (2020).
[15] K. Varga, R. G. Lovas, and R. J. Liotta, Phys. Rev. Lett. **69**, 37 (1992).
[16] G. Röpke, P. Schuck, Y. Funaki, H. Horiuchi, Z. Ren, A. Tohsaki, C. Xu, T. Yamada, and B. Zhou, Phys. Rev. C **90**, 034304 (2014).
[17] C. Xu, Z. Ren, G. Röpke, P. Schuck, Y. Funaki, H. Horiuchi, A. Tohsaki, T. Yamada, and B. Zhou, Phys. Rev. C **93**, 011306(R) (2016).
[18] C. Xu, G. Röpke, P. Schuck, Z. Ren, Y. Funaki, H. Horiuchi, A. Tohsaki, T. Yamada, and B. Zhou, Phys. Rev. C **95**, 061306(R) (2017).
[19] S. Yang, C. Xu, G. Röpke, P. Schuck, Z. Ren, Y. Funaki, H. Horiuchi, A. Tohsaki, T. Yamada, and B. Zhou, Phys. Rev. C **101**, 024316 (2020).
[20] S. Yang, C. Xu, and G. Röpke, Phys. Rev. C **104**, 034302 (2021).
[21] S. M. S. Ahmed, R. Yahaya, S. Radiman, and M. S. Yasir, J. Phys. G **40**, 065105 (2013).
[22] S. M. S. Ahmed, R. Yahaya, S. Radiman, M. S. Yasir, H. A. Kassim, and M. U. Khandaker, Eur. Phys. J. A **51**, 13 (2015).
[23] D. Deng, Z. Ren, D. Ni, and Y. Qian, J. Phys. G **42**, 075106 (2015).
[24] D. Deng and Z. Ren, Phys. Rev. C **93**, 044326 (2016).
[25] B. Buck, A. C. Merchant, and S. M. Perez, At. Data Nucl. Data Tables **54**, 53 (1993).

[26] B. Buck, A. C. Merchant, and S. M. Perez, Phys. Rev. Lett. **72**, 1326 (1994).
[27] B. Buck, J. C. Johnston, A. C. Merchant, and S. M. Perez, Phys. Rev. C **53**, 2841 (1996).
[28] S. A. Gurvitz and G. Kalbermann, Phys. Rev. Lett. **59**, 262 (1987).
[29] G. Royer and R. A. Gherghescu, Nucl. Phys. A **699**, 479 (2002).
[30] D. S. Delion, S. Peltonen, and J. Suhonen, Phys. Rev. C **73**, 014315 (2006).
[31] D. S. Delion and R. J. Liotta, Phys. Rev. C **87**, 041302(R) (2013).
[32] C. Xu and Z. Ren, Phys. Rev. C **74**, 037302 (2006).
[33] C. Xu and Z. Ren, Nucl. Phys. A **753**, 174 (2005); Phys. Rev. C **73**, 041301(R) (2006).
[34] C. Xu and Z. Ren, Phys. Rev. C **74**, 014304 (2006); **78**, 057302 (2008).
[35] C. Xu and Z. Ren, Phys. Rev. C **76**, 027303 (2007).
[36] D. Ni and Z. Ren, Phys. Rev. C **80**, 014314 (2009).
[37] Y. B. Qian and Z. Ren, Nucl. Phys. A **852**, 82 (2011).
[38] N. Wan, C. Xu, and Z. Ren, Phys. Rev. C **92**, 024301 (2015).
[39] D. Ni and Z. Ren, Phys. Rev. C **93**, 054318 (2016).
[40] J. Fan and C. Xu, Nucl. Phys. A **989**, 1 (2019).
[41] J. Liu, R. Xu, J. Zhang, C. Xu, and Z. Ren, J. Phys. G **46**, 055105 (2019).
[42] K. P. Santhosh, J. G. Joseph, and S. Sahadevan, Phys. Rev. C **82**, 064605 (2010).
[43] K. P. Santhosh and C. Nithya, Phys. Rev. C **94**, 054621 (2016).
[44] K. P. Santhosh, D. T. Akrawy, H. Hassanabadi, A. H. Ahmed, and T. A. Jose, Phys. Rev. C **101**, 064610 (2020).
[45] F. Mercier, J. Zhao, R. D. Lasseri, J. P. Ebran, E. Khan, T. Nikšić, and D. Vretenar, Phys. Rev. C **102**, 011301(R) (2020).
[46] R. D. Macfarlane and A. Siivola, Phys. Rev. Lett. **14**, 114 (1965).
[47] E. Roeckl, R. Kirchner, O. Klepper, G. Nyman, W. Reisdorf, D. Schardt, K. Wien, and R. Fass, and S. Mattsson, Phys. Lett. B **78**, 393 (1978).
[48] D. Schardt, R. Kirchner. O. Klepper, W. Reisdorf, E. Roeckl, P. Tidemand-Petersson, G. T. Ewan, E. Hagberg, B. Jonson, S. Mattsson, and G. Nyman, Nucl. Phys. A **326**, 65 (1979).
[49] D. Schardt, T. Batsch, R. Kirchner, O. Klepper, W. Kurcewicz, E. Roeckl, and P. Tidemand-Petersson, Nucl. Phys. A **368**, 153 (1981).
[50] Z. Janas, C. Mazzocchi, L. Batist, A. Blazhev, M. Górska, M. Kavatsyuk, O. Kavatsyuk, R. Kirchner, A. Korgul, M. La Commara, K. Miernik, I. Mukha, A. Płochocki, E. Roeckl, and K. Schmidt, Eur. Phys. J. A **23**, 197 (2005).
[51] D. Seweryniak, K. Starosta, C. N. Davids, S. Gros, A. A. Hecht, N. Hoteling, T. L. Khoo, K. Lagergren, G. Lotay, D. Peterson, A. Robinson, C. Vaman, W. B. Walters, P. J. Woods, and S. Zhu, Phys. Rev. C **73**, 061301(R) (2006).
[52] I. G. Darby, R. K. Grzywacz, J. C. Batchelder, C. R. Bingham, L. Cartegni, C. J. Gross, M. Hjorth-Jensen, D. T. Joss, S. N. Liddick, W. Nazarewicz, S. Padgett, R. D. Page, T. Papenbrock, M. M. Rajabali, J. Rotureau, and K. P. Rykaczewski, Phys. Rev. Lett. **105**, 162502 (2010).
[53] S. N. Liddick, R. Grzywacz, C. Mazzocchi, R. D. Page, K. P. Rykaczewski, J. C. Batchelder, C. R. Bingham, I. G. Darby, G. Drafta, C. Goodin, C. J. Gross, J. H. Hamilton, A. A. Hecht, J. K. Hwang, S. Ilyushkin, D. T. Joss, A. Korgul, W. Królas, K. Lagergren, K. Li *et al.*, Phys. Rev. Lett. **97**, 082501 (2006).
[54] K. Auranen, D. Seweryniak, M. Albers, A. D. Ayangeakaa, S. Bottoni, M. P. Carpenter, C. J. Chiara, P. Copp, H. M. David, D. T. Doherty, J. Harker, C. R. Hoffman, R. V. F. Janssens, T. L. Khoo, S. A. Kuvin, T. Lauritsen, G. Lotay, A. M. Rogers, J. Sethi, C. Scholey *et al.*, Phys. Rev. Lett. **121**, 182501 (2018).
[55] Y. Xiao, S. Go, R. Grzywacz, R. Orlandi, A. N. Andreyev, M. Asai, M. A. Bentley, G. de Angelis, C. J. Gross, P. Hausladen, K. Hirose, S. Hofmann, H. Ikezoe, D. G. Jenkins, B. Kindler, R. Léguillon, B. Lommel, H. Makii, C. Mazzocchi, K. Nishio *et al.*, Phys. Rev. C **100**, 034315 (2019).
[56] F. G. Kondev, M. Wang, W. J. Huang, S. Naimi, and G. Audi, Chin. Phys. C **45**, 030001 (2021).
[57] W. J. Huang, M. Wang, F. G. Kondev, G. Audi, and S. Naimi, Chin. Phys. C **45**, 030002 (2021).
[58] M. Wang, W. J. Huang, F. G. Kondev, G. Audi, and S. Naimi, Chin. Phys. C **45**, 030003 (2021).
[59] C. F. Weizsäcker, Eur. Phys. J. A **96**, 431 (1935).
[60] H. A. Bethe and R. F. Bacher, Rev. Mod. Phys. **8**, 82 (1936).
[61] W. D. Myers and W. J. Swiatecki, Nucl. Phys. **81**, 1 (1966).
[62] J. Duflo and A. P. Zuker, Phys. Rev. C **52**, R23 (1995).
[63] G. Royer and A. Subercaze, Nucl. Phys. A **917**, 1 (2013).
[64] P. Möller, A. J. Sierk, T. Ichikawa, and H. Sagawa, At. Data Nucl. Data Tables **109**, 1 (2016).
[65] N. Wang, M. Liu, X. Z. Wu, and J. Meng, Phys. Lett. B **734**, 215 (2014).
[66] G. F. Bertsch, J. Borysowicz, H. Mcmanus, and W. G. Love, Nucl. Phys. A **284**, 399 (1977).
[67] G. R. Satchler and W. G. Love, Phys. Rep. **55**, 183 (1979).
[68] A. M. Kobos, B. A. Brown, P. E. Hodgson, G. R. Satchler, and A. Budzanowski, Nucl. Phys. A **384**, 65 (1982).
[69] J. D. Walecka, *Theoretical Nuclear Physics and Subnuclear Physics* (Oxford University Press, Oxford, 1995).
[70] B. Hahn, D. G. Ravenhall, and R. Hofstadter, Phys. Rev. **101**, 1131 (1956).
[71] A. Bohr and B. R. Mottelson, *Nuclear Structure*, Vol. 1 (World Scientific, Singapore, 1998).
[72] Z. Ren and G. Xu, Phys. Rev. C **36**, 456 (1987).
[73] Z. Ren and G. Xu, J. Phys. G **15**, 465 (1989).